Riemannian Geometric Approaches for Measuring Movement Quality

Anirudh Som, Rushil Anirudh, Qiao Wang, Pavan Turaga

School of Electrical, Computer and Energy Engineering, Arizona State University
School of Arts, Media and Engineering, Arizona State University

Abstract

A growing set of applications in home-based interactive physical therapy require the ability to monitor, inform and assess the quality of everyday movements. Interactive therapy requires both real-time feedback of movement quality, as well as summative feedback of quality over a period of time. Obtaining labeled data from trained experts is the main limitation, since it is both expensive and time consuming. Motivated by recent studies in motor-control, we propose an unsupervised approach that measures movement quality of simple actions by considering the deviation of a trajectory from an ideal movement path in the configuration space. We use two different configuration spaces to demonstrate this idea – the product space $\mathcal{S}^1 \times \mathcal{S}^1$ to model the interaction of two joint angles, and $SE(3) \times SE(3)$ to model the movement of two joints, for two different applications in movement quality estimation. We also describe potential applications of these ideas to assess quality in real-time.

1. Introduction

In many applications for health-care, the ability to monitor, inform, and asses the quality of our movements, plays a key role. This ability can enable the creation of systems that one could use on an everyday basis while reducing the time and effort required on the part of trained physical therapist. Home based systems are also more intimate, and reduce the need to travel elsewhere for physical therapy. A growing class of affordable sensing devices have led to the development of such home-based and hospital-based systems that can provide feedback and quality ratings for movements. Sensors for motion capture (e.g. Optitrack, Microsoft Kinect), accelerometers and gyroscopes are often used in such systems. Similar ideas are also being studied in the context of sports and athletics [15].

In the effort to build autonomous systems, a large body of work combines features obtained from the sensor data

with machine learning techniques to predict quality scores similar to a physical therapist/experts. This involves obtaining labeled data from therapists, which is used to train a model [5, 20, 15, 18]. Obtaining such labels are not easy, since domain knowledge is very essential in most applications for movement quality assessment. Additionally, physical therapists ratings are often very subjective, with wide variability in rating across different therapists. One approach to decouple the inherent subjectivity of rating vs true quality is via a combination of crowd-sourcing platforms such as Amazon MTurk [1], with computational methods such as non-negative matrix factorization. This approach has been difficult to pursue in fields where experts are required to label data such as in physical therapy and medical imaging, and where sharing of patient data raises many concerns.

In this paper, we consider the role of geometric constraints in human body, and associated metrics for measuring movement quality. We base our approach on recent studies which suggest that the most efficient movement between two poses, in certain well defined cases, is often the geodesic path in the pose-space [4]. Some of these results have been reported in other forms, such as showing that the optimal reaching movements in the Euclidean space appear curved [3, 11]. Recent work in motor control suggests that, when presented with visual feedback of the configuration space of two joints (more specifically, a torus), as applied to a reaching movement, subjects' movements tend to converge to geodesics on the torus [7].

These results suggest that the geometry of the configuration space may have an important role to play in creating effective, scalable algorithms for a variety of applications in interactive rehabilitation and physical therapy. While the basic scientific results reviewed above suggest a clear unifying framework in terms of optimal paths and geodesics, there are several engineering research problems that arise in practical implementation. Firstly, in order to create a general algorithmic framework, one needs to have a modular approach to plug in different kinds of configuration spaces as available from different sensing modalities: such
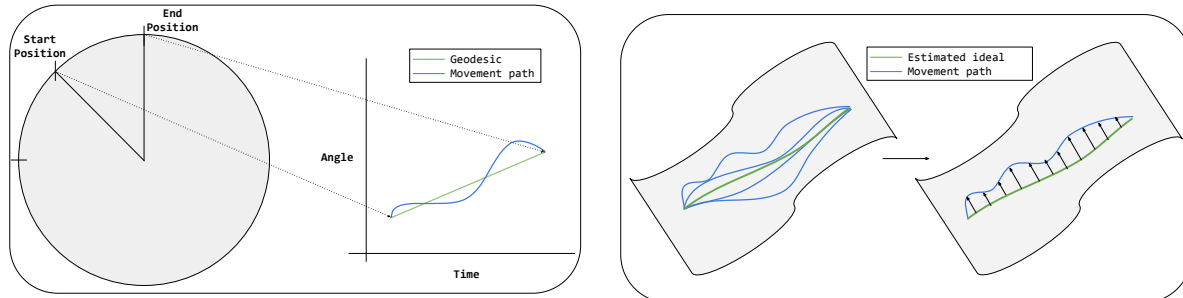
(a) Comparing simple movements to the samples along the geodesic.

(b) For more complex movements that require temporal segmentation, we estimate the mean as the ideal path.

Figure 1. We propose to measure movement quality as the deviation of a given trajectory w.r.t. an ideal path, for movements on $\mathcal{S}^1 \times \mathcal{S}^1$, and $SE(3) \times SE(3)$.

as product-space of circles for joint angles obtained from motion-capture devices, or shape silhouettes from video sensors. Secondly, one needs effective computational approaches to measure quality in real-time to enable their use in an interactive setting (e.g. interactive movement therapy). Thirdly, a study of the correlation between geometrically derived measures of quality, with other clinical measures of quality such as those obtained from force plates etc. is needed to throw light on the possibility of using them as surrogates of clinical measures. We consider two cases where we show promising results for quality analysis of human movement – 1) movement quality of the sit-to-stand (STS) actions, where we consider the important feature to be opening of the hip angle, measured on the left and right side and is represented on the product space of circles, $\mathcal{S}^1 \times \mathcal{S}^1$, and 2) reaching movements in stroke rehabilitation [5], where we represent the skeleton of the upper body as a point on $SE(3) \times SE(3)$, and its correlation with clinical measures of reaching quality. An overview of our approach is presented in figures 1a and 1b.

Contributions:

1. We propose to model the deviation of a given trajectory w.r.t. an ideal path, on a pose-space as a measure of quality: applied to the specific case of $\mathcal{S}^1 \times \mathcal{S}^1$ and $SE(3) \times SE(3)$ in two different applications.

2. We evaluate our approach and study the correlations between our quality measures with other clinical movement quality measures.

3. We also present a framework for real-time approximations of quality as the movement is being executed, for potential use in an interactive therapy system.

2. Related Work

Assessing the quality of everyday actions has tremendous scope in applications like sports, healthcare rehabilitation systems, exercise systems, retrieval of videos and so

on. There have been several efforts to evaluate the performance of specific actions by using trajectory-based evaluation metrics [8, 10, 14]. Recent work has investigated the use of spatio-temporal pose features from video segments, for estimating quality of sports actions, such as diving and figure-skating [15]. This is based on learning a regression function from pose-features to quality scores, which does not give much insight into what constitutes good movement quality. Another line of work, in the field of stroke rehab therapy, the computational score is made more intuitive by breaking into interpretable components for assessment of reach movements of stroke survivors [21]. However, this analysis requires pre-specification of components from domain knowledge, and may not generalize to other domains.

Dynamical system theory and geometric techniques have also been employed for analysis of movement quality. Shape distribution functions of the reconstructed phase space have been used for classifying movements of unimpaired/healthy and stroke-impaired subjects [20]. This approach also requires training sets for regressing shape distributions to movement quality. Recently, Tao *et al.* [18] developed a method for online movement quality assessment of gait movement via hidden Markov modeling of normal movements using Kinect skeleton data. Both these approaches require machine learning methodologies, and generally lack interpretability.

3. Mathematical Preliminaries

Here, we describe the geometric properties of the two spaces we consider in this paper – $\mathcal{S}^1 \times \mathcal{S}^1$ and the space of $SE(3) \times SE(3)$.

3.1. Body-joint angles on $\mathcal{S}^1 \times \mathcal{S}^1$

For this study, we consider the hip angles on the left and right side of the body as shown in figure 2. The reason for using the left and right sides of the hip is to incorporate the symmetry of the action. It has been observed that symmetrical distribution of body weight under the feet, significantly
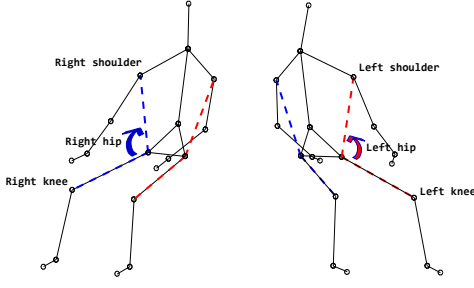
Figure 2. Illustration of the hip angles computed on the left and right side of the body, for the sit-to-stand experiment.

improves STS actions in subjects suffering from hemiplegic stroke [6]. In other studies, improvements in postural stance was found to be correlated to postural symmetry as well [24].

Each of these angles can be represented equivalently on the circle, $\mathcal{S}^1$, and the angles computed from both the left and right side can be represented in the product space $\mathcal{S}^1 \times \mathcal{S}^1$ which is the torus T^2. This space possesses a Riemannian structure obtained by inheriting the Riemannian metric from $\mathbb{R}^2$ on the circle $\mathcal{S}^1 \subset \mathbb{R}^2$.

Although the geodesics are inherited from the geodesic on $\mathcal{S}^1$, the actual metric on T^2 is a design choice. We will use a simple combination of the sum of the length of the shortest arc on the individual circles as our metric. This distance is defined as $d : \mathcal{S}^1 \times \mathcal{S}^1 \to \mathbb{R}$

$$d_{\mathcal{S}}(\theta_1, \theta_2) = \arccos(\cos(\theta_1 - \theta_2)), \quad (1)$$

Next, the distance on the torus between points $p_1 = (\phi_1, \theta_1)$ and $p_2 = (\phi_2, \theta_2)$ is given by $d_T(p_1, p_2) = \sqrt{d_{\mathcal{S}}^2(\phi_1, \phi_2) + d_{\mathcal{S}}^2(\theta_1, \theta_2)}$.

3.2. Product space of the special Euclidean group

For the stroke rehabilitation experiment, we represent a stick figure as a combination of relative transformations between joints [19]. The resulting feature for each skeleton is interpreted as a point on the product space of $SE(3) \times SE(3)$. These transformation matrices lie on the curved space known as the Special Euclidean group $SE(3)$. Therefore the set of all transformations lies on the product space of $SE(3) \times SE(3)$.

The special Euclidean group, denoted by $SE(3)$ is a Lie group, containing the set of all 4×4 matrices of the form

$$P(R, \overrightarrow{d}) = \begin{bmatrix} R & \overrightarrow{d} \\ 0 & 1 \end{bmatrix}, \quad (2)$$

where R denotes the rotation matrix, which is a point on the special orthogonal group $SO(3)$ and $\overrightarrow{d}$ denotes the translation vector, which lies in $\mathbb{R}^3$. The 4×4 identity matrix

I_4 is an element of $SE(3)$ and is the identity element of the group. The tangent space of $SE(3)$ at I_4 is called its Lie algebra – denoted here as $\mathfrak{se}(3)$. It can be identified with 4×4 matrices of the form

$$\widehat{\xi} = \begin{bmatrix} \widehat{\omega} & \overrightarrow{v} \\ 0 & 0 \end{bmatrix} = \begin{bmatrix} 0 & -\omega_3 & \omega_2 & v_1 \\ \omega_3 & 0 & -\omega_1 & v_2 \\ -\omega_2 & \omega_1 & 0 & v_3 \\ 0 & 0 & 0 & 0 \end{bmatrix}, \quad (3)$$

where $\widehat{\omega}$ is a 3×3 skew-symmetric matrix and $\overrightarrow{v} \in \mathbb{R}^3$. An equivalent representation is $\xi = [\omega_1, \omega_2, \omega_3, v_1, v_2, v_3]^T \in \mathbb{R}^6$. We are following the notation to denote the vector space ($\xi \in \mathbb{R}^6$) and the equivalent Lie algebra representation ($\widehat{\xi} \in \mathfrak{se}(3)$) as [13] (pg. 411). The exponential and inverse exponential maps are given below for completeness [13] (pg. $413 - 414$). The exponential map is given by

$$\exp \widehat{\xi} = \begin{bmatrix} I & \overrightarrow{v} \\ 0 & 1 \end{bmatrix} \; \omega = 0 \text{ and } \exp \widehat{\xi} = \begin{bmatrix} e^{\widehat{\omega}} & A\overrightarrow{v} \\ 0 & 1 \end{bmatrix} \; \omega \neq 0, \quad (4)$$

where $e^{\widehat{\omega}}$ is given explicitly by the Rodrigues' formula –
$= I + \frac{\widehat{\omega}}{\|\omega\|}\sin\|\omega\| + \frac{\widehat{\omega}^2}{\|\omega\|^2}(1 - \cos\|\omega\|)$, and $A = I + \frac{\widehat{\omega}}{\|\omega\|^2}(1 - \cos\|\omega\|) + \frac{\widehat{\omega}^2}{\|\omega\|^3}(\|\omega\| - \sin\|\omega\|)$. The inverse exponential map is given by

$$\widehat{\xi} = \log \begin{bmatrix} R & d \\ 0 & 1 \end{bmatrix} = \begin{bmatrix} \widehat{\omega} & A^{-1}d \\ 0 & 0 \end{bmatrix}, \quad (5)$$

where $\widehat{\omega} = \log R$, and

$$A^{-1} = I - \frac{1}{2}\widehat{\omega} + \frac{2\sin\|\omega\| - \|\omega\|(1 + \cos\|\omega\|)}{2\|\omega\|^2\sin\|\omega\|}\widehat{\omega}^2 \quad \omega \neq 0,$$

when $\omega = 0$, then $A = I$.

4. Measures of Quality

In this section, we outline two complementary approaches to quantify movement quality. The first one is a summative measure, which requires observing the full trajectory of movement. The other is a online version for potential use in real-time feedback, which is based on sequentially accumulating the deviation from an idealized trajectory, thereby not requiring full observation of the trajectory. Both these approaches easily generalize to both geometric spaces under consideration.

Also, the framework is quite general in its treatment of what is the 'idealized' movement. In the absence of additional information, we represent the ideal movement as the geodesic between start and end poses, in the respective representation space. However, for more complex movements, a geodesic may be an oversimplification of the ideal movement. Instead, one may need to average several trajectories obtained form healthy subjects to define the ideal. Given a

large enough dataset for the given movement that are segmented in time, the average trajectory can be computed using tools developed, as in Su *et al.* [17].

4.1. Summative quality measure

The idea of summative quality centers around measuring the deviation of a given trajectory compared to an idealized trajectory. This idealized trajectory could be a simple geodesic or a more complex trajectory computed by averaging a few 'normal' trajectories. To keep things simple, we will make it specific to the torus, where the idealized trajectory is fixed to the geodesic between the start and the end pose.

The geodesic on a circle is the shortest arc that connects two points, where the metric is defined as in (1). In order to compare a movement trajectory with the geodesic, we must first sample along the geodesic. Let $\gamma(t)$ represent the trajectory for which we wish to estimate a quality score. Further, let $\widetilde{\gamma}(t)$ represent the geodesic path with the same starting and ending points as $\gamma(t)$, i.e., $\gamma(0) = \widetilde{\gamma}(0)$ and $\gamma(1) = \widetilde{\gamma}(1)$. Let us then define the geodesic discretization interval to be given by $\delta = \frac{d_\mathcal{S}(\gamma(1),\gamma(0))}{N-1}$, where N is the number of desired samples along $\gamma(t)$. Since our operations are on the circle, $\mathcal{S}^1$, we are able to uniformly sample along the geodesic using δ as $\widetilde{\gamma}(t) = \gamma(0) + (t\,\delta)$.

$L = \gamma(0) - \gamma(1)$, at 'time' t, the sampled geodesic is given by

$$\widetilde{\gamma}(t) = \begin{cases} \gamma(0) + (t\,\delta), & \text{if } (L > \pi) \text{ or } (-\pi < L < 0) \\ \gamma(0) - (t\,\delta), & \text{else.} \end{cases}$$

$$(6)$$

Once the angles for both the original and geodesic trajectory have been computed, we solve the registration problem between the two trajectories using Dynamic Time Warping (DTW) [12]. The deviation from geodesic measure (DGM) obtained using DTW is used as the final quality score, which is given by $q = \text{DTW}(\gamma_\phi, \widetilde{\gamma}_\phi) + \text{DTW}(\gamma_\theta, \widetilde{\gamma}_\theta)$. Where γ_θ and γ_ϕ refer to the movement trajectories corresponding to first and second angles, θ and ϕ, respectively. For the STS experiment, we use the above approach. Given more data of 'ideal' movements, we can replace the geodesic $\widetilde{\gamma}$ by the mean sequence [17].

4.2. Towards an online quality measure

While summative feedback is useful to assess quality, it is also imperative for interactive feedback systems to generate real-time movement quality as the movement is being executed. Summative measure as defined above requires observing the full movement. In this section, we outline a strategy to obtain an approximate measure of deviation that can be implemented in a real-time setting as the movement is evolving. Movement quality is measured by the deviation from the *ideal* movement. The deviation for each new point

along a trajectory is represented as the tangent vector

$$v(t) = \log_{\widetilde{\gamma}(t)} \gamma(t), \quad q(t) = \|v(t)\| \qquad (7)$$

We propose to use $q(t)$ as the basis of our online quality score. The intuition being that a larger tangent vector implies a bigger deviation from the average trajectory, and therefore a poor quality of movement. The feature $q(t)$ can be used to drive feedback in real-time, since the average trajectory is obtained offline as part of training. In order to incorporate temporal information, we cumulate scores over time to produce the score at time instant T, i.e. $q(T) = \sum_t q(t)$.

Su *et al.* [17] proposed a representation to allow metrics that are invariant to speed. They also propose an algorithm to compute the mean of a set of trajectories, after they have been aligned in time. In a real-time setting, this is difficult to perform, since we only have access to the previous few frames. In this paper, we assume that the movements have been registered in time following which we extract the features per frame to show its effectiveness in capturing quality information. An alternative way work around this problem could be to fit splines [16] or geodesics [9] to the data directly, which can work for both repetitive and non-repetitive movements.

5. Experimental results

We validate the proposed approach for movement quality estimation on two different experimental conditions: 1) STS actions of four healthy subjects, 2) Reach and grasp actions of 19 stroke survivors.

5.1. Sit-to-stand quality assessment

In this experiment, the data set was provided to us by the authors of [22]. The data set was collected using a Microsoft Kinect sensor and consists of the 3D position information of the 20 body joints for four healthy subjects. Each of the subjects was first asked to perform a few STS actions in their normal habitual manner. Next, each subject was asked to practice with the system for 10 minutes after being given few verbal instructions. The subjects were instructed to perform the STS actions in a relaxed, smooth manner, with their head guiding the whole body. They were also instructed to make sure that they moved forward and up at the same time. These STS actions come under the control (CT) stage. After resting for an hour, each subject was again asked to practice with the system for 10 minutes, but this time with auditory feedback and these STS action come under the feedback (FB) stage. On a whole, each subject carried out 12 STS actions during the CT stage and 21 STS actions during the FB stage. For subject 2, we show results for only 9 STS actions in CT and 21 STS actions in FB, due to data recording problems. The findings reported

in [22], indicate that the quality performance of all the four subjects generally improved with practice. The improvement was also greater when auditory feedback was present. Since there are no ground truth scores in this data set, we propose to generate quality scores for each movement, and show that our measures depict the same trend reported in [22] which is – movement quality becomes better with practice.

We compute the angles between the left and right: shoulder, hip and knee joints, denoted by θ and ϕ respectively as illustrated in figure 2. This ensures that the postural symmetry of the subject is considered while calculating the quality score. The final DGM score is computed using the distance metric defined in (1) between the movement trajectory and the corresponding geodesic path, as described in section 4.1. A smaller DGM score is indicative of a well executed STS movement and a higher score indicates a poorer quality of movement.

The results of this experiment are shown in figure 4. We show the quality scores across all STS movements carried out by each of the 4 subjects. To better indicate the trends for each subject, we also show the least squares fit line for the CT stage, FB stage and across all the STS sessions. We see no improvement for Subjects 2 and 3 during the CT stage as shown by the CT line fit. However, both subjects improve their movements during the FB stage as shown by the FB line fit. Subjects 1 and 4 show lower quality scores as the number of sessions in the CT stage progresses and continue to improve their movements during the FB stage as well. Figures 5 and 6 show an example of the variation of the geodesic and original trajectory with time and on the $\mathcal{S}^1 \times \mathcal{S}^1$ representation space, for both the CT and FB stage respectively. On the whole, all four subjects show a tendency to learn while performing the STS actions with each progressing session as clearly seen from the total line fit plot for each subject. These results follow the same trend reported in [22]. Summary of the trends of the DGM score and the metrics used in [22] can be seen in Table 1.

Table 1. Summary of the percentage change of the average movement quality measurements from the CT stage to the FB stage, for each of the 4 subjects. Decrease in the values for DGM score, Two-peak coefficient (TPC), and increase in the values for minimum hip angle correspond to improvement in movement quality.

Movement Quality Measure	S1	S2	S3	S4
DGM score (%)	-51	-5.6	-29	-34
TPC of head speed (%)	-56	-25	-75	-25
Minimum hip angle (%)	6.8	9.8	19	4.2

5.2. Reach assessment in stroke rehabilitation

Stroke leaves millions of patients disabled with reduced motor function, which severely restricts a person's ability to perform activities of daily living. As a result, there is a strong effort to design home systems that can provide feedback and enable survivors to improve their motor function over time, while reducing the costs typically incurred by a typical physical therapy session. We use data collected by the system developed by Chen *et al.* [5]. The system uses 14 markers to analyze and study the patient's movement (eg. reach and grasp), usually in the presence of a therapist who then provides a movement quality score, such as the Wolf Motor Function Test (WMFT) [23].

The goal of experiments such as this, is to predict the quality of the stroke survivor's movement as well as the WMFT score. Particularly, we are interested in unsupervised quality measures, which reduces the need to obtain labeled data. There are 14 markers on the right hand, arm and torso in a hospital setting. A total of 19 impaired subjects perform multiple repetitions of reach and grasp movements, both on-table and elevated (with the additional force of gravity acting against their movement). Each subject performs 4 sets of reach and grasp movements to different target locations, with each set having 10 repetitions. The dataset is collected in "sessions" consisting of multiple movements. As a result, the proposed measure is meaningless unless temporal segmentation is performed first as in the previous experiment. Instead, we choose a bottom-up approach, where we estimate the ideal trajectory as the mean of all the movements in the dataset. We use the quality score as explained in section 4.2.

We use the feature settings as described in [2]. This is used to represent the hand joints in relative configurations to each other as is done in LARP [19] resulting in each hand skeleton as a point in $SE(3) \times SE(3)$. In order to compare our scores, we report the ranked correlation values against the WMFT [23] scores on the day of recording, where a therapist evaluates the subject's ability on a scale of 1 - 5 (with 5 being least impaired to 1 being most impaired).

Table 2 and figure 3 show the performance of the proposed approaches as they correlate with the WMFT score on movement quality. We obtain a correlation coefficient of

Table 2. Comparison of the correlation scores between the proposed movement quality measure in $SE(3)$, to other unsupervised quality measures.

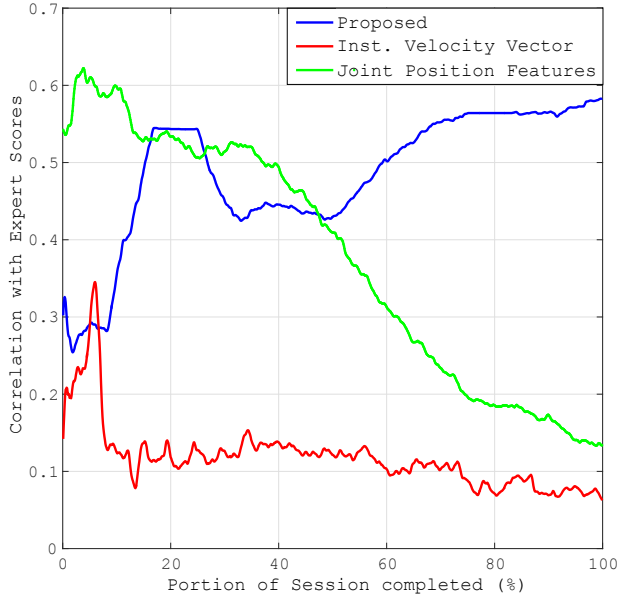| Movement Quality Measure	Correlation
Proposed	**0.5832**
Inst. velocity vector magnitude on $SE(3)$	0.0625
Joint position features	0.1341

Figure 3. Unsupervised online movement quality estimation: Performance of the proposed quality score at each time instant is shown here, which given by the correlation coefficient with the WMFT scores given by an expert. Our method is able to take in new information with time, to give better performance.

0.5832 with the WMFT score and a p-value of 3×10^{-8}. It is important to note that while better results have been reported with other features [20, 2], these are usually supervised approaches and require training. These methods also cannot be used in an online setting. Figure 3 shows the correlation score as a function of time, where we estimate the quality score in an online fashion. As we observe more of the movement, we are able to predict the quality better. Here, we compute the shooting vector at each frame that goes from $v(t) = \log_{\mu(t)}(\gamma(t))$, the magnitude of the vector is the quality score for that time instant. We accumulate these features by adding them from all the previous frames. We compare with a similar score extracted from joint position features in R^3, which performs poorly. We also compare with magnitude of the instantaneous velocity, extracted for each frame as $\|v(t)\| = \|\log_{\gamma(t-1)}(\gamma(t))\|$. It is interesting to note that among the three features, ours is the only one that is able to accumulate quality information accurately, so that our estimate gets better with time. At each time instant, after we estimate the quality score, we perform a correlation with the WMFT scores to compute the performance which is reported in figure 3.

6. Conclusion and Future Work

We proposed an unsupervised framework that uses the deviation from the ideal path of a trajectory in an appropriate pose-space, to measure movement quality. We apply the methodology to STS movements, interpreted as a curve on the torus, $\mathcal{S}^1 \times \mathcal{S}^1$, and for reaching movements interpreted as a curve on $SE(3) \times SE(3)$. Our experimental results look promising and show the effectiveness of the proposed framework. This points the way toward more complex full-body quality assessments, that could utilize geodesicness measures on general shape manifolds. The DGM quality score can also be generalized to include true elastic invariant metrics such as those developed by Su *et. al.* [17].

References

[1] Amazon Mechanical Turk. https://www.mturk.com/mturk/welcome. Accessed: 16-11-2013. 1

[2] R. Anirudh, P. Turaga, J. Su, and A. Srivastava. Elastic functional coding of Riemannian trajectories. *Accepted at IEEE transactions on Pattern Analysis and Machine Intelligence, April*, 2016. 5, 6

[3] F. Arce, I. Novick, M. Shahar, Y. Link, C. Ghez, and E. Vaadia. Differences in context and feedback result in different trajectories and adaptation strategies in reaching. *PLoS One*, 4(1):e4214, 2009. 1

[4] A. Biess, D. G. Liebermann, and T. Flash. A computational model for redundant human three-dimensional pointing movements: integration of independent spatial and temporal motor plans simplifies movement dynamics. *The Journal of Neuroscience*, 27(48):13045–13064, 2007. 1

[5] Y. Chen, M. Duff, N. Lehrer, H. Sundaram, J. He, S. L. Wolf, T. Rikakis, T. D. Pham, X. Zhou, H. Tanaka, et al. A computational framework for quantitative evaluation of movement during rehabilitation. In *AIP Conference Proceedings-American Institute of Physics*, volume 1371, page 317, 2011. 1, 2, 5

[6] P.-T. Cheng, S.-H. Wu, M.-Y. Liaw, A. M. Wong, and F.-T. Tang. Symmetrical body-weight distribution training in stroke patients and its effect on fall prevention. *Archives of physical medicine and rehabilitation*, 82(12):1650–1654, 2001. 3

[7] Z. Danziger and F. A. Mussa-Ivaldi. The influence of visual motion on motor learning. *The Journal of Neuroscience*, 32(29):9859–9869, 2012. 1

[8] A. S. Gordon. Automated video assessment of human performance. In *Proceedings of AI-ED*, pages 16–19, 1995. 2

[9] Y. Hong, N. Singh, R. Kwitt, and M. Niethammer. Time-warped geodesic regression. In *Medical Image Computing and Computer-Assisted Intervention–MICCAI 2014*, pages 105–112. Springer, 2014. 4

[10] M. Jug, J. Perš, B. Dežman, and S. Kovačič. Trajectory based assessment of coordinated human activity. *3rd International Conference on Computer Vision Systems (ICVS)*, 2626:534–543, 2003. 2

[11] K. M. Mosier, R. A. Scheidt, S. Acosta, and F. A. Mussa-Ivaldi. Remapping hand movements in a novel geometrical environment. *Journal of neurophysiology*, 94(6):4362–4372, 2005. 1

[12] M. Müller. Dynamic time warping. In *Information retrieval for music and motion*, chapter 4, pages 69–84. Springer, 2007. 4
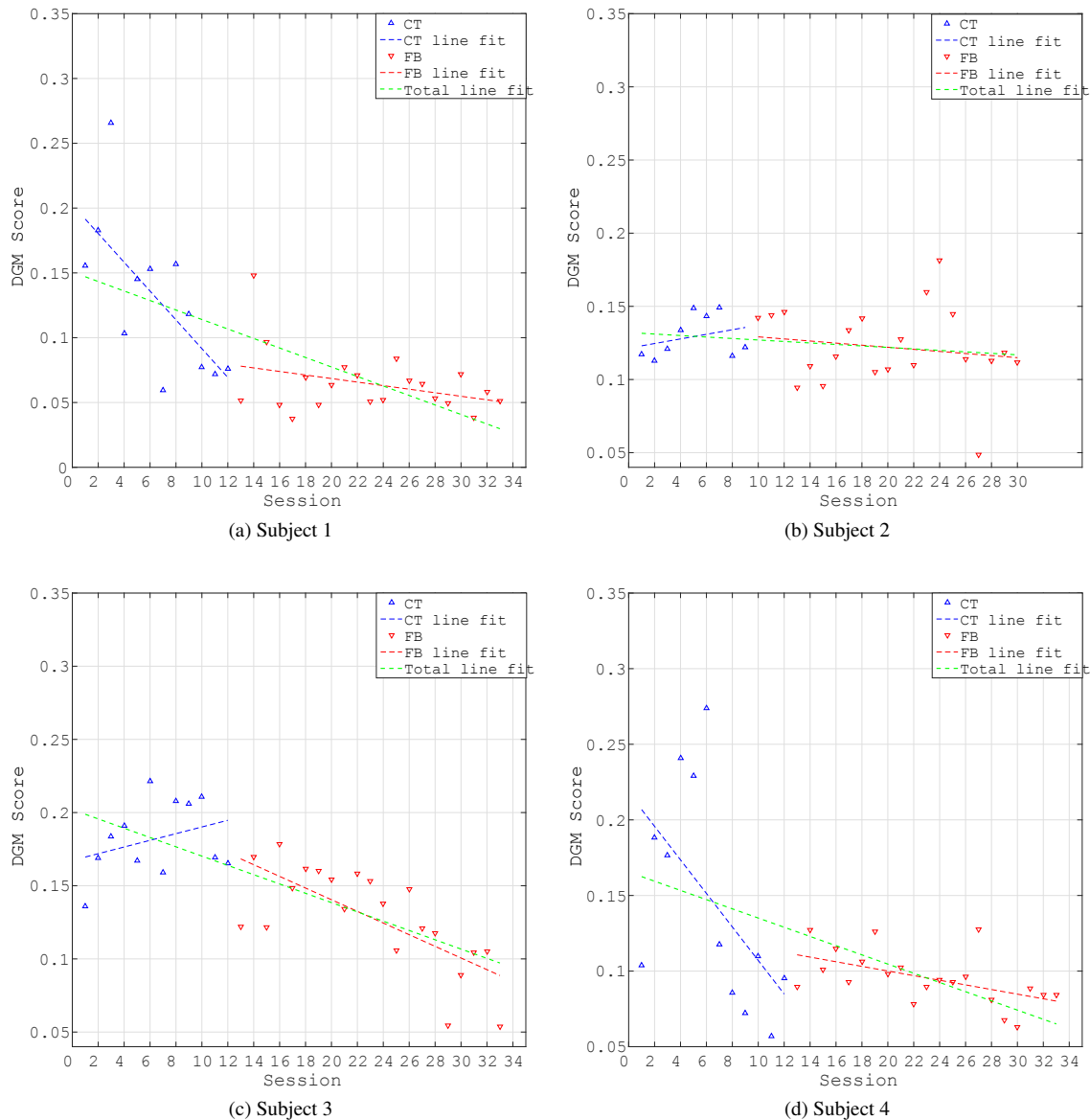
Figure 4. **Lower score is better.** For the STS dataset, we show movement quality scores during 30 - 33 sessions for 4 subjects. The trends seen here, indicate the change in quality of motion with practice. CT indicates the control group receiving no feedback, FB indicates the group receiving feedback to enable better movement. The downward trend is clearly visible, similar to the results reported in [22]

[13] R. M. Murray, Z. Li, S. S. Sastry, and S. S. Sastry. *A mathematical introduction to robotic manipulation*. CRC press, 1994. 3

[14] M. Perše, M. Kristan, J. Perš, and S. Kovačič. Automatic evaluation of organized basketball activity using bayesian networks. *Computer Vision Winter Workshop (CVWW)*, pages 11–18, 2007. 2

[15] H. Pirsiavash, C. Vondrick, and A. Torralba. Assessing the quality of actions. In *Computer Vision–ECCV 2014*, pages 556–571. Springer, 2014. 1, 2

[16] J. Su, I. L. Dryden, E. Klassen, H. Le, and A. Srivastava. Fitting smoothing splines to time-indexed, noisy points on non-

linear manifolds. *Image and Vision Computing*, 30(6):428–442, 2012. 4

[17] J. Su, S. Kurtek, E. Klassen, and A. Srivastava. Statistical analysis of trajectories on Riemannian manifolds: Bird migration, hurricane tracking, and video surveillance. *Annals of Applied Statistics*, 8(1), 2014. 4, 6

[18] L. Tao, A. Paiement, D. Aldamen, M. Mirmehdi, S. Hannuna, M. Camplani, T. Burghardt, and I. Craddock. A comparative study of pose representation and dynamics modelling for online motion quality assessment. *Computer Vision and Image Understanding*, November 2015. 1, 2

[19] R. Vemulapalli, F. Arrate, and R. Chellappa. Human action
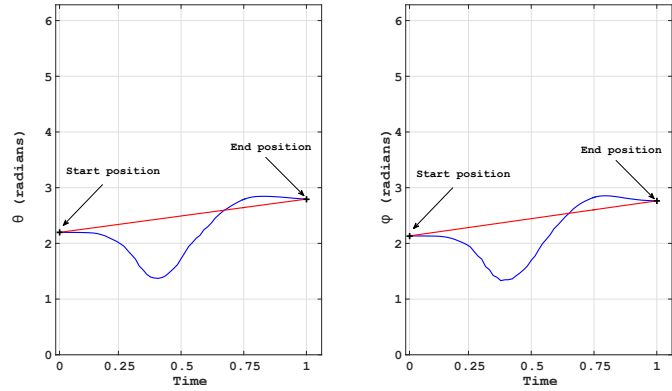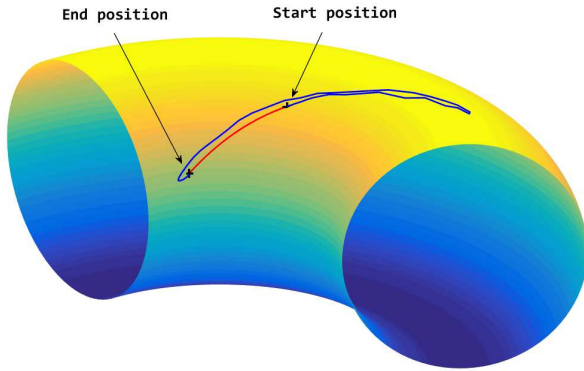
(a) STS action on the $\mathcal{S}^1 \times \mathcal{S}^1$ configuration space.

(b) Variation of individual joint angles with time.

Figure 5. Representation of the subject's movement vs geodesic formed using the joints angles θ and ϕ, for a STS session carried out during the CT stage, with no feedback. θ represents the joint angle between the left-shoulder, left-hip and left-knee; ϕ represents the joint angle between the right-shoulder, right-hip and right-knee. The trajectory shown with blue represents the original trajectory and the trajectory shown with red represents the geodesic. The DGM quality score was equal to 0.22127, indicating a relatively low match to the geodesic, i.e. a low quality movement.
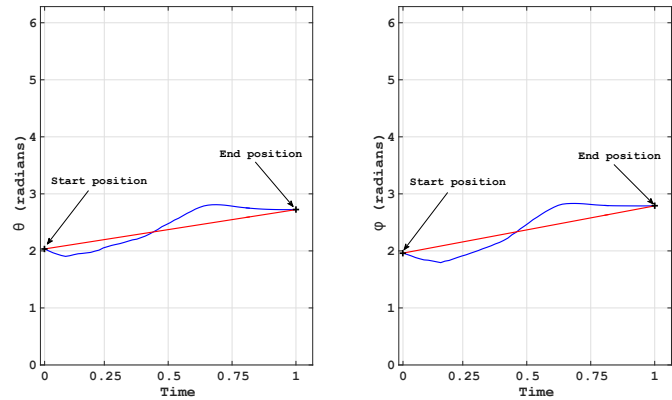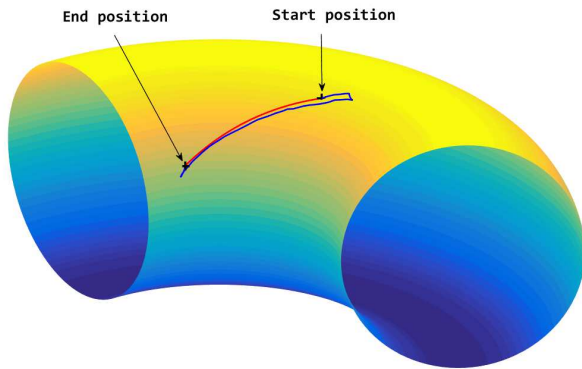
(a) STS action on the $\mathcal{S}^1 \times \mathcal{S}^1$ configuration space.

(b) Variation of individual joint angles with time.

Figure 6. Representation of the subject's movement vs geodesic formed using the joints angles θ and ϕ, for a STS session carried out during the FB stage. θ represents the joint angle between the left-shoulder, left-hip and left-knee; ϕ represents the joint angle between the right-shoulder, right-hip and right-knee. The trajectory shown with blue represents the original trajectory and the trajectory shown with red represents the geodesic. The proposed DGM quality score was equal to 0.048226, indicating a close match to the ideal geodesic, i.e. a high quality movement.

recognition by representing 3d skeletons as points in a lie group. In *CVPR, 2014*, pages 588–595, June 2014. 3, 5

[20] V. Venkataraman and P. Turaga. Shape descriptions of non-linear dynamical systems for video-based inference. *IEEE Transactions on Pattern Analysis and Machine Intelligence*, PP(99):1–1, 2016. 1, 2, 6

[21] V. Venkataraman, P. Turaga, M. Baran, N. Lehrer, T. Du, L. Cheng, T. Rikakis, and S. L. Wolf. Component-level tuning of kinematic features from composite therapist impressions of movement quality. *IEEE Journal of Biomedical and Health Informatics*, 20(1):143–152, January 2014. 2

[22] Q. Wang, P. Turaga, G. Coleman, and T. Ingalls. Somatech:

an exploratory interface for altering movement habits. In *CHI'14 Extended Abstracts on Human Factors in Computing Systems*, pages 1765–1770. ACM, 2014. 4, 5, 7

[23] S. L. Wolf, P. A. Catlin, M. Ellis, A. L. Archer, B. Morgan, and A. Piacentino. Assessing wolf motor function test as outcome measure for research in patients after stroke. *Stroke*, 32(7):1635–1639, 2001. 5

[24] A. M. Wong, L. Ming-Yih, K. Jung-Kun, and T. Fuk-Tan. The development and clinical evaluation of a standing biofeedback trainer. *Journal of rehabilitation research and development*, 34(3):322, 1997. 3